Electric Power Systems Research 209 (2022) 107935

Contents lists available at ScienceDirect

Electric Power Systems Research

journal homepage: www.elsevier.com/locate/epsr

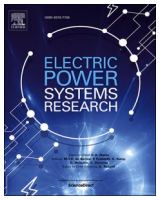

Modeling and open source implementation of balanced and unbalanced harmonic analysis in radial distribution networks

Tomislav Antić [*,a], Leon Thurner [b], Tomislav Capuder [a], Ivica Pavić [a]

[a] Department of Energy and Power Systems, Faculty of Electrical Engineering and Computing, University of Zagreb, Zagreb, Croatia
[b] retoflow GmBH, Kassel, Germany

ARTICLE INFO

Keywords:
Harmonic analysis modeling
Open source development
Pandapower
Radial distribution networks

ABSTRACT

With the increasing integration of new technologies, power system operators are facing new operational and planning challenges. Most of these changes are caused by power electronics devices of low carbon (LC) units, resulting in more frequent violations of limits defined in the standards, such as the unwanted occurrence of higher-order harmonics. These aspects indicate that an open source tool, capable of analyzing and estimating future impacts of the above-mentioned phenomena and technologies, would be of great benefit. The paper presents the development of a Phyton-based open source tool as an extension of the existing pandapower library. The upgrade includes the capability of balanced and unbalanced harmonic analysis for LC impact assessment. The technical background and mathematical formulations implemented in the newly developed tool are explained in detail and benchmarked against existing commercial tools showing high accuracy, i.e., the median deviation between the results calculated by the developed and the commercial tool is no larger than 0.21% in the worst-case scenario. In addition to verification, the developed tool is used for the analysis of a real-world network with a high share of LC technologies. The source code of the tool is made available for verification and future updates.

1. Introduction

1.1. Motivation

The installed capacity of the renewable energy sources is continuously growing [1]. Besides the capacity of large power plants connected to the transmission network, the installed capacity of smaller distributed generators (DGs), e.g., PV power plants have increased [2]. The decrease in prices has made the PVs more available to the end-users, leading to a high installed capacity in low-voltage networks, which in some countries can be 70% of total PV capacity [3]. Since the price of other low-carbon (LC) technologies, e.g., battery storage [4], is also decreasing, it is expected that the share of LC technologies will be significantly higher than it is today. Even though some of LC technologies can provide ancillary services and help in the operation of the power system [5], others can lead to voltage [6] and congestion problems [7], increased harmonic distortion [8], voltage unbalance [9], and other unwanted events. Since the share of LC technologies is not expected to fall, it is important to develop adequate tools that can easily assess the impact of LC technologies on power quality (PQ) parameters in a power system. Most of LC units' interfaces to the power system are through power electronic devices and, in addition to a higher share of nonlinear loads, the increased harmonic distortion is becoming an increasing challenge for distribution system operators. Unknown or unallowed values of harmonic distortion can lead to serious problems in the planning and operation of power systems, such as increased thermal losses, tripping of protection, overheating of transformers windings, and decrease in performance.

1.2. Literature review

The assessment of the LC technologies' impact on PQ parameters is a well-known problem and numerous papers have dealt with mitigating one or more problems related to a PQ or other problems in power systems. Research is done using licensed, commercial tools, or open source tools [10–12].

The authorsuthors of paper[13] use NEPLAN for load flow (LF) with load profiles analysis. NEPLAN was used as a tool for assessing the impact of optimal investment decisions from distributed energy resources planning tools on local electricity networks [14]. The same tool was also used for the detection of overvoltages and reverse power flows

* Corresponding author.
E-mail addresses: tomislav.antic@fer.hr (T. Antić), leon.thurner@retoflow.de (L. Thurner), tomislav.capuder@fer.hr (T. Capuder), ivica.pavic@fer.hr (I. Pavić).

https://doi.org/10.1016/j.epsr.2022.107935
Received 29 October 2021; Received in revised form 12 February 2022; Accepted 16 March 2022
Available online 22 March 2022

Nomenclature

$[\Delta U_{\{\}/abc,h}]$ h th order harmonic voltage/phase harmonic voltage drop vector of the power system
$[U_{\{\}/abc,h}]$ h th order harmonic voltage/phase harmonic voltage vector of the power system
$[U_{abc,r/n,h}]$ h th order harmonic phase voltage vector of the referent node r/node n in the unbalanced network
$[Y_{012/abc,\ k,l}]$ sequence/phase admittance matrix of the element between nodes k,l
$[Y_{012/abc/\{\}}]$ sequence/phase/balanced admittance matrix of the observed network
$[Z_{012/abc,r,h}]$ sequence/phase impedance matrix of the referent node r for the hth harmonic
$[Z_{abc/\{\},\{\}/h}]$ phase/balanced impedance matrix of the observed network for the fundamental/hth harmonic
$\delta_{0/1,e}$ angle of the zero/positive sequence impedance of the external grid
$\frac{X_{0,e}}{X_{1,e}}$ external grid's zero sequence to positive sequence reactance
$\frac{X_{0/1,e}}{R_{0/1,e}}$ external grid's zero/positive sequence resistance to reactance ratio
$\varphi_{\{\}/p,n,s,h}$ angle of the harmonic current of the harmonic source s connected three-phase symmetrically/to the phase p to the node n
$\theta_{\{\}/p,n,s,h}$ defined hth order angle of the harmonic current of the harmonic source s connected three-phase symmetrically/to the phase p to the node n
c voltage factor
$I_{\{\}/p,n,s,h}$ h th order harmonic current of the harmonic source s connected three-phase symmetrically/to the phase p to the node n
$i_{\{\}/p,n,s,h}$ defined hth order harmonic current of the harmonic source s connected three-phase symmetrically/to the phase p to the node n expressed as the percentage of the fundamental harmonic
$I_{\{\}/p,r,h}$ h th order harmonic current of the referent node r connected three-phase symmetrically/to the phase p
$R_{0/1\ k,l}$ zero/positive sequence resistance of the element between nodes k,l
$R_{0/1,e}$ zero/positive sequence resistance of the external grid
S_B base apparent power
$S_{\{\}/p,n}$ power of the load/generator connected to the node n/phase p of the node n
S''_{SC} three-phase short circuit power
$THD_{i,p,n}$ total current harmonic distortion of the phase p of the node n
$THD_{u,p,n}$ total voltage harmonic distortion of the phase p of the node n
U_n nominal voltage
$U_{0/1/2,n}$ zero/positive/negative sequence voltage of the node n
$U_{\{\}/p,n,1}$ voltage of the phase p of the node n
$U_{r/n,h}$ h th order harmonic voltage of the referent node r/node n in the balanced network
$X_{0/1\ k,l}$ zero/positive sequence reactance of the element between nodes k,l
$X_{0/1,e,h}$ zero/positive sequence reactance of the external grid for the hth harmonic
$X_{L/C,h}$ inductive/capacitive reactance for the hth harmonic
$Y_{0/1/2\ k,l}$ zero/positive/negative sequence admittance of the element between nodes k,l
$Z_{0/1,e,h}$ zero/positive sequence impedance of the external grid for the hth harmonic
$Z_{0/1/2\ k,l}$ zero/positive sequence impedance of the element between nodes k,l
$Z_{0/1/2,e,h,p.u.}$ zero/positive/negative sequence impedance of the external grid for the hth harmonic
$|Z_{0/1,e}|$ magnitude of the zero/positive sequence impedance of the external grid
$|I_{\{\}/p,n,s,h}|$ magnitude of the harmonic current of the harmonic source s connected three-phase symmetrically/to the phase p to the node n

caused by the PV [15].

The optimal penetration level of PV systems in the distribution network considering both power loss reduction and protection miscoordination cost to maximize the profit of the Distribution System Operator is determined using ETAP [16]. The paper [17] presents the effect of an EV parking lot equipped with a roof-mounted PV type solar power plant on the distribution network along with the simulations in the ETAP environment considering physical location limitations. ETAP is used for the LF analysis and the short circuit calculation as a preprocess to the proposal of the combined fuse and numerical relays inter-linked with digital logic-based adaptive overcurrent protection scheme [18].

DigSILENT PowerFactory is used for the voltage stability analysis of the simplified distribution feeder in time domain simulations [19]. In [20], a reactive power-voltage-based framework to evaluate the voltage instability sensitivities of power system buses with the increase in renewable energy penetration has been developed using DigSILENT PowerFactory for performing the simulations of the test grid. Effects of increasing solar connections which are realistic in near future have been analyzed by modeling the detailed network in DigSILENT PowerFactory simulation platform [21].

The above-mentioned and other commercial power system analysis tools are often used because of their reliability, different analyses possibilities, intuitiveness, and other numerous advantages. However, they are often expensive, and since they are licensed, it is not always easy to automatize the processes or to connect them with other tools. Therefore the number of power system analyses made by using open source tools is growing.

Thurner et al. [22] describe pandapower, an open source Python tool, used for automation of static and quasi-static analysis and optimization of both balanced and unbalanced systems. The implementation of IEC 60909 short circuit calculation in pandapower was presented another paper that describes the mathematical formulation behind the tool's development [23]. The same tool was used for the reconfiguration of a distribution network, where pandapower elements and functions were used in finding an optimal topology based on a reinforcement learning approach [24].

Zimmerman et al. [25] present MATPOWER, an open source Matlab-based power system analysis tool, similar to pandapower, which can be used for different network analyses. Balanced LF functionality of MATPOWER is used for solving the problem of unit commitment and economic dispatch in microgrids [26]. The combination of speed of MATPOWER and the search capabilities of a meta-heuristic optimization algorithm was used to find the optimal location of an electric vehicle charging station in a local microgrid [27].

OpenDSS, an open source tool specialized in unbalanced power systems, can be used for power flow and harmonic LF analyses, whose results are the input for optimal energy scheduling and a power quality

improvement of a microgrid [28]. OpenDSS is also usedto investigate the synergy between uncontrolled charging of plug-in EVs and the energy generation from wind-based DGs [29]. The authors in paper [30] use OpenDSS software for power flow analysis and the evaluation of voltage unbalance, steady-state voltage, and transformer load for the assessment of the potential benefits the connection of PVs can bring to a commercial building with EV charging stations.

Most open source tools are validated against commercial ones and show differences no larger than 0.08% [31,32]. Therefore, they are often used in simulations of power systems. Since they are free and do not require expensive licenses, they can be used in automatized processes, can easily be connected with external databases, and combined with other tools. Most importantly, the open source approach allows easier further upgrade and development. However, open source tools often do not have the same analytical capability compared to commercial tools, the methodology is often not documented, their use often requires programming capabilities, whereas commercial tools have graphical user interfaces.

1.3. Contributions

Even though the mathematical formulation of both balanced and unbalanced harmonic analysis is a well-known problem, defined and described in detail in numerous papers [33–36], such papers only present mathematical models, and often lack verification and application of the presented model. Additionally, this paper presents a summarized and detailed mathematical formulation for harmonic analyses in both balanced and unbalanced radial distribution networks. The mathematical model can be used in further implementations of harmonic assessment but also as a basis for the upgrade of the developed tool. Since most of the tools lack the information about the implementation of the mathematical model used in different analyses, this paper enables a better understanding of the idea behind the implementation. The detailed mathematical model also enables easier defining of needed input data when using the tool in different harmonic analyses. Despite the existence of papers that present the results of harmonic calculations and analyses based on open source tools [28,37,38], none of them give a detailed mathematical model of harmonic analysis, and they are often not verified against other software, which can make the correctness of results questionable. In addition, even though they are free to use, their formulation is not publicly available and they cannot be further upgraded. To overcome all the above-mentioned issues, a harmonic analysis tool developed as an extension of the pandapower Python-based open source tool is presented in this paper. A detailed mathematical background, used as a basis for the development is presented in detail. Also, the developed tool is validated on both balanced and unbalanced radial distribution networks against NEPLANand DigSILENT PowerFactory commercial tools. To additionally emphasize the benefits and possibilities of the developed tool, a real-world LV network with a high share of EVs is analyzed with harmonic time series simulations, using the developed tool. The developed tool is also publicly available and can be accessed at any time [39], which makes any possible further upgrades easier to implement.

The rest of the paper is organized as follows: Section 2 briefly introduces the detailed mathematical background and the methodology with explained equations used for the calculation of harmonics-related values. Section 3 presents the verification of the developed tool on several test networks. To additionally show the potential and the importance of the developed tool, a real-world network with different scenarios defining the share of PVs and EV charging stations is analyzed in a case study defined in Section 4. Finally, Section 5 highlights the conclusions and plans for future upgrades of the developed tool.

2. Mathematical background and modeling

2.1. Impedance matrix

To calculate THD_u, higher-order harmonic voltages of the referent node and all other nodes must be calculated. The first step of the development of the open source tool is the calculation of the impedance matrix since harmonic voltages are calculated using the impedance matrix for each frequency and harmonic currents at each node. The same step is needed for LF calculations both in balanced and unbalanced power systems. In the case of unbalanced networks, the creation of an impedance matrix is possible by using sequence components or by using a three-phase approach. Since a lot of the LV network data, acquired from the DSO, is given with sequence values, authors in paper [40] define sequence matrix for both power systems with grounded and without grounded neutral voltage. The sequence matrix can be used in further calculations or it can be transformed into the phase impedance matrix, depending on the needs or representation preferences.

The parameters of the lines in the distribution systems are defined with the resistance and the reactance of the positive and zero systems. The resistance and the reactance of the positive and the negative system are the same for passive power system elements, such as lines and transformers. The impedance of the positive and zero system of the element (e.g., transformer or line) that connects nodes k and l is calculated using (1) and (2).

$$Z_{1\ k,l} = R_{1\ k,l} + jX_{1\ k,l}\ [\Omega] \tag{1}$$

$$Z_{0\ k,l} = R_{0\ k,l} + jX_{0\ k,l}\ [\Omega] \tag{2}$$

$$[Y_{012\ k,l}] = \begin{bmatrix} Y_{0\ k,l} & 0 & 0 \\ 0 & Y_{1\ k,l} & 0 \\ 0 & 0 & Y_{2\ k,l} \end{bmatrix} \tag{3}$$

$$[Y_{abc\ k,l}] = [A]^{-1}[Y_{012\ k,l}][A] \tag{4}$$

$$[A] = \begin{bmatrix} 1 & 1 & 1 \\ 1 & a^2 & a \\ 1 & a & a^2 \end{bmatrix} \quad \text{where } a = 1\angle 120^{\circ} \tag{5}$$

The newly developed tool relies on already developed pandapower functions such as that of creating sequence admittance matrices Y_0, Y_1, and Y_2 in per-unit values. Created matrices are valid for the whole observed network and admittance between every two elements of the network can be extracted. The first row and column of each matrix are removed since they present the admittance between referent and other nodes.

Matrix $Y_{012\ k,l}$ is created for each element of matrices Y_0, Y_1, and Y_2 as shown in (3). Using (4) and (5), the sequence admittance matrix is transformed to the phase admittance matrix $Y_{abc\ k,l}$.

From each created $Y_{abc\ k,l}$ matrix the Y_{abc} matrix of the entire network is created (6). The dimension of the matrix is $3\cdot(n-1) \times 3\cdot(n-1)$ since the rows and columns related to the referent node are removed.

$$[Y_{abc}] = \begin{bmatrix} Y_{aa\ 1,1} & Y_{ab\ 1,1} & Y_{ac\ 1,1} & \dots & Y_{aa\ 1,n} & Y_{ab\ 1,n} & Y_{ac\ 1,n} \\ Y_{ba\ 1,1} & Y_{bb\ 1,1} & Y_{bc\ 1,1} & \dots & Y_{ba\ 1,n} & Y_{bb\ 1,n} & Y_{bc\ 1,n} \\ Y_{ca\ 1,1} & Y_{cb\ 1,1} & Y_{cc\ 1,1} & \dots & Y_{ca\ 1,n} & Y_{cb\ 1,n} & Y_{cc\ 1,n} \\ \vdots & \vdots & \vdots & \ddots & \vdots & \vdots & \vdots \\ Y_{aa\ n,1} & Y_{ab\ n,1} & Y_{ac\ n,1} & \dots & Y_{aa\ n,n} & Y_{ab\ n,n} & Y_{ac\ n,n} \\ Y_{ba\ n,1} & Y_{bb\ n,1} & Y_{bc\ n,1} & \dots & Y_{ba\ n,n} & Y_{bb\ n,n} & Y_{bc\ n,n} \\ Y_{ca\ n,1} & Y_{cb\ n,1} & Y_{cc\ n,1} & \dots & Y_{ca\ n,n} & Y_{cb\ n,n} & Y_{cc\ n,n} \end{bmatrix} \tag{6}$$

After the phase admittance matrix is created, the phase impedance matrix Z_{abc} is calculated as the inverse of the admittance matrix (7).

$$[Z_{abc}] = [Y_{abc}]^{-1} \tag{7}$$

When a balanced, symmetrical network is observed, there is no need to calculate a three-phase or sequence component matrix. The

impedance matrix is calculated using only the positive system values of the lines (1). By using pandapower functionalities, it is possible to get the admittance matrix in per unit values (8). Since the model of the harmonic calculation presented in this paper uses the impedance matrix, the Y matrix (8) needs to be inverted (9).

$$[Y] = \begin{bmatrix} Y_{1,1} & \cdots & Y_{1,n} \\ \vdots & \ddots & \vdots \\ Y_{n,1} & \cdots & Y_{n,n} \end{bmatrix} \tag{8}$$

$$[Z] = [Y]^{-1} \tag{9}$$

2.2. Voltage and current harmonic distortion

The impedance matrices calculation defined in 2.1 are valid for a base frequency of 50 Hz. To calculate higher-order harmonics, the impedance matrix must be determined for each frequency at which the harmonic distortion is calculated. It is assumed that the resistance of the elements does not change with the frequency, since in distribution networks, especially in LV networks, the dependence on the frequency is not as expressed as in the transmission networks. In most of the European standards which define limitations for distribution networks, higher-order harmonics are defined for a maximum of 2 kHz. For frequencies so high, neglecting a frequency-resistance dependence will not significantly affect the accuracy of the model. The inductive reactance changes with the frequency, according to (10) and (11). In case when the reactive capacitance is known, it changes according to (12) and (13). Mentioned equations are valid for modeling each element defined with the resistance and the reactance.

$$X_{L,h} = 2\cdot\pi\cdot 50\,\text{Hz}\cdot h\cdot L \tag{10}$$

$$X_{L,h} = h\cdot X_{L,1} \tag{11}$$

$$X_{C,h} = \frac{1}{2\cdot\pi\cdot 50\,\text{Hz}\cdot h\cdot C} \tag{12}$$

$$X_{C,h} = \frac{X_{C,1}}{h} \tag{13}$$

According to Ćuk et al. [41] transformers can be represented with an equivalent series RL model for lower frequencies, i.e., the reactance of a transformer can be calculated using (10) and (11). Similar to lines, the frequency dependency of the transformer's resistance can be neglected. Both for lines and transformers, the frequency dependency of the resistance can be considered by accurate [42] or simple, approximate models [43]. Initially, different models were implemented in the tool, and simulations were made using those models. However, the results have shown the detailed model does not significantly improve the accuracy of the developed tool. Hence, it is omitted in the final version of the algorithm.

Eqs. (10) –(13) are used for the positive, the negative, and the zero system sequence, with values valid for each of the sequence systems. Since the assumption in this paper is that the resistance does not change with the frequency, from the resistance at the fundamental frequency (50 Hz) and the admittance at each non-fundamental frequency, a three-phase impedance matrix is calculated for every observed higher-order harmonic, according to the Eqs. (1)–(7). In the case of a balanced network, the logic of calculating an impedance matrix remains the same for every higher-order harmonic, and a matrix is determined by using Eqs. (1), (8) and (9).

After the impedance matrix is calculated, the nodal current of each node n (for the balanced systems analyses) or the current of each phase p of the node n (for unbalanced systems analyses) needs to be calculated. The node current is calculated from the apparent power of the load/generator $S_{n,s}$ connected to the node and the node voltage U_n (14), which is the result of the LF calculation. When the network is unbalanced, the harmonic current of each phase p of the observed node n is calculated from the apparent power of the load/generator $S_{n,p,s}$ connected to the phase p of the node n and the node phase voltage $U_{n,p}$ (15), which is the result of the unbalanced LF calculation. Every load/generator is a harmonic source, injecting the harmonic current into the network. If a generator or a load in the analysis does not inject the harmonic current it can be defined with the current of zero amperes for each higher-order harmonic. The power and the voltage are per-unit values. Therefore, the calculated current is also a per-unit value. Using per-unit values in the mathematical formulation is of great benefit, due to the possibility of determining harmonic problems in networks with multiple voltage levels. It is particularly important due to the penetration of RES in distribution networks and bi-directional power flows, as otherwise, the system operators would not be able to analyze multiple voltage levels.

$$I_{n,s,1} = \frac{S_n^*}{\sqrt{3}\cdot U_{n,1}} \tag{14}$$

$$I_{p,n,s,1} = \frac{S_{p,n}^*}{U_{p,n,1}} \tag{15}$$

Since both the power and the voltage are complex numbers, the harmonic current of the node is also defined as a complex number and it can be presented in the polar form. Most devices that cause harmonic distortion are considered as harmonic sources and are defined with the harmonic spectra consisting of magnitude and phase angle. Also, the values of voltages in LF calculations are described with magnitude and phase angles. Therefore, it is common to use the polar form instead of the Cartesian form. Eq. (16) presents the polar form of the hth order harmonic current of the node n, and the harmonic source s in case of a balanced network, i.e., $|I_{n,s,h}|$ is the higher-order harmonic current magnitude and $\angle\varphi_{n,s,h}$ is the phase angle of the same current. When a network is unbalanced, the hth harmonic order current of the node n is calculated for each phase p and each harmonic source s (17).

$$I_{n,s,h} = |I_{n,s,h}|\angle\varphi_{n,s,h} \tag{16}$$

$$I_{p,n,s,h} = |I_{p,n,s,h}|\angle\varphi_{p,n,s,h} \tag{17}$$

Both nodal and phase current are obtained from the base frequency current calculation, the percentage, and the phase angle of the higher-order frequencies. The percentage of the higher-order frequency is defined as the share of the hth order harmonic current in the fundamental harmonic. Both the percentage and the phase angle are defined as input parameters of the harmonic calculation, and they need to be defined for every element that injects harmonic current into a network. When a network is balanced, the harmonic analysis can be done by taking into consideration only the positive sequence system or by considering positive, negative, and zero sequence systems.

When only positive sequence is considered, the nodal current of the hth order harmonic and the harmonic source s is calculated according to (18)–(20). When calculating higher-order harmonics, only the magnitude of the fundamental harmonic current is considered, since in most cases the current of fundamental harmonic is defined with the percentage value of 100% that represents the magnitude and without the angle.

$$I_{n,s,h} = |I_{n,s,1}|\cdot i_{n,s,h}\angle\left(h\cdot\theta_{n,s,h} + 240^\circ\right) \tag{18}$$

$$|I_{n,s,h}| = |I_{n,s,1}|\cdot i_{n,s,h} \tag{19}$$

$$\angle\varphi_{n,s,h} = h\cdot\theta_{n,s,h} + 240^\circ \tag{20}$$

The detailed methodology and the logic behind the implementation of Eqs. (16)–(20) are presented in Xu [33], Modeling [34]. These equations are basic equations needed for the harmonic analysis model described in this paper. Moreover, as defined in Xu [33], this model is the most common one used in commercial power system harmonic analysis programs and is therefore used in the development of the open

source harmonic analysis program.

When the system is balanced, and all three sequence systems are observed, the current is calculated depending on the harmonic order. Under the balanced situation, the positive sequence components can be used to represent the balanced harmonic component with order $h = 3{\cdot}m + 1$, the negative sequence component can be used when the harmonic order is $h = 3{\cdot}m + 2$, and the zero sequence can be used when the harmonic order is $h = 3{\cdot}m$, as defined in Zheng et al. [44], Manjure and Makram [45]. In the case when all sequence systems are observed magnitudes of harmonic currents are calculated the same as in the case when only the positive sequence system is considered (19), and angles of the harmonic currents are calculated using equations defined in (21).

$$\angle\varphi_{n,s,h} = \begin{cases} h{\cdot}\theta_{n,s,h} & , \ h = 3{\cdot}m \\ h{\cdot}\theta_{n,s,h} + 240^{\circ} & , \ h = 3{\cdot}m + 1 \\ h{\cdot}\theta_{n,s,h} + 120^{\circ} & , \ h = 3{\cdot}m + 2 \end{cases} \tag{21}$$

When the three-phase unbalanced radial distribution network is observed, the calculation of the harmonic angles needs to be modified since all sequence systems have an impact in determining the angles of the harmonic currents. Angle φ of each phase p of node n and the harmonic source s for the hth order harmonic is calculated with Eqs. (22)–(24). The calculation of phase angles in harmonic analysis of unbalanced radial distribution networks is just an extension of the equations valid for balanced distribution networks defined in Zheng et al. [44], Manjure and Makram [45].

$$\varphi_{a,n,s,h} = \angle\left(h{\cdot}\theta_{a,n,s,h}\right) \forall h \tag{22}$$

$$\varphi_{b,n,s,h} = \begin{cases} h{\cdot}\theta_{b,n,s,h} & , \ h = 3{\cdot}m \\ h{\cdot}\theta_{b,n,s,h} + 240^{\circ} & , \ h = 3{\cdot}m + 1 \\ h{\cdot}\theta_{b,n,s,h} + 120^{\circ} & , \ h = 3{\cdot}m + 2 \end{cases} \tag{23}$$

$$\varphi_{c,n,s,h} = \begin{cases} h{\cdot}\theta_{c,n,s,h} & , \ h = 3{\cdot}m \\ h{\cdot}\theta_{c,n,s,h} + 120^{\circ} & , \ h = 3{\cdot}m + 1 \\ h{\cdot}\theta_{c,n,s,h} + 240^{\circ} & , \ h = 3{\cdot}m + 2 \end{cases} \tag{24}$$

In case when there are S different harmonic sources connected to the same node n, the resulting hth order nodal harmonic current is calculated as the sum of harmonic currents injected by every harmonic source s, as shown in Eqs. (25) and (26).

$$I_{n,h} = \sum_{s=1}^{S} I_{n,s,h} \tag{25}$$

$$I_{p,n,h} = \sum_{s=1}^{S} I_{p,n,s,h} \tag{26}$$

Since the impedance matrix and harmonic current injections are determined both for balanced and unbalanced power systems, the system harmonic voltage drop is calculated by direct solution of the linear Eqs. (27) and (28), both for balanced and unbalanced networks [46].

$$[\Delta U_h] = [Z_h]{\cdot}[I_h] \tag{27}$$

$$[\Delta U_{abc\ h}] = [Z_{abc\ h}]{\cdot}[I_{abc\ h}] \tag{28}$$

When a balanced network is observed, and the impact of the zero and the negative sequence system cannot be neglected, the direct solution of the linear Eq. (27) needs to be modified. Since the positive sequence and the negative sequence impedance are set to be equal, in the case of the harmonic order $h = 3{\cdot}m + 1$ or $h = 3{\cdot}m + 2$, the impedance matrix created using only the positive sequence values can be used in voltage drop calculations for those harmonics. However, when the harmonic order is $h = 3{\cdot}m$, $[Z_h]$ used in (28) must be created with only zero sequence values, same as in (8) and (9). Even when the harmonic order is $h = 3{\cdot}m$, the mathematical model for the calculation of harmonic voltage drop remains the same. The only difference is that the elements in the impedance matrix are defined with zero sequence values.

In order to calculate the higher-order harmonic voltage of each node, it is necessary to calculate the voltage of the referent node for each of the higher-order harmonics. Similar to calculating the voltage drop, the impedance and the current of the referent node must be determined to calculate the voltage. The positive sequence impedance of the external grid in per-unit values is defined with Eqs. (29)–(34). Voltage factor c is used as a parameter in calculating the impedance of an external grid. It is used in short-circuit calculations in order to scale the equivalent voltage source. Since the impedance of an external grid is calculated from the three-phase short-circuit power, it is used in the calculations. Depending on the case, the value of the factor can vary between 0.95 and 1.1. In the examples presented in this paper, the used value is equal to 1, but it can be changed when using the tool, according to the user's preferences.

$$|Z_{1,e}| = c{\cdot}\frac{U_n^2}{S''_{SC}} \tag{29}$$

$$\delta_1 = \arctan\frac{X_{1,e}}{R_{1,e}} \tag{30}$$

$$R_{1,e} = |Z_{1,e}|{\cdot}\cos\delta_1 \tag{31}$$

$$X_{1,e} = |Z_{1,e}|{\cdot}\sin\delta_1{\cdot}h \tag{32}$$

$$Z_{1,e,h} = R_{1,e} + j{\cdot}X_{1,e,h} \tag{33}$$

$$Z_{1,e,h,\ p.u.} = Z_{1,e,h}{\cdot}\frac{S_B}{U_n^2} \tag{34}$$

In cases of harmonic analyses, the impedance of zero sequence needs to be determined for the referent node voltage calculation. The zero sequence impedance is calculated according to the Eqs. (35)–(40).

$$|Z_{0,e}| = |Z_{1,e}|{\cdot}\frac{X_{0,e}}{X_{1,e}} \tag{35}$$

$$\delta_0 = \arctan\frac{X_{0,e}}{R_{0,e}} \tag{36}$$

$$R_{0,e} = |Z_{0,e}|{\cdot}\cos\delta_1 \tag{37}$$

$$X_{0,e} = |Z_{0,e}|{\cdot}\sin\delta_1{\cdot}h \tag{38}$$

$$Z_{0,e,h} = R_{0,e} + j{\cdot}X_{0,e,h} \tag{39}$$

$$Z_{0,e,h,\ p.u.} = Z_{0,e,h}{\cdot}\frac{S_B}{U_n^2} \tag{40}$$

The calculation of an external grid's impedance and other parameters important for harmonic analysis is defined with Eqs. (29)–(40). These equations are used in different power system analyses, e.g., short-circuit calculations, and a similar form of the described mathematical model is used in commercial tools such as NEPLAN or Power Factory.

When a distribution network is balanced, and all three sequence systems are considered, then the harmonic impedance of the referent node is equal to the harmonic impedance of the external grid positive sequence impedance (34) when $h = 3{\cdot}m + 1$ or $h = 3{\cdot}m + 2$, and is equal to the harmonic impedance of the external grid's zero sequence impedance (40) when $h = 3{\cdot}m$. When the zero and the negative systems are neglected, no matter the harmonic order, the harmonic impedance of the referent node is equal to the harmonic impedance of the external grid's positive sequence impedance (34).

For an unbalanced network, once the positive and the zero sequence impedance are calculated, the nodal sequence impedance matrix is created (41), with the assumption that the positive and negative sequence impedance are the same. Since the voltage drop is calculated for each phase and not for sequence systems, the sequence impedance matrix is transformed to the phase impedance matrix for each harmonic

order h using (42).

$$[Z_{012,r,h}] = \begin{bmatrix} Z_{0,e,h,\ p.u.} & 0 & 0 \\ 0 & Z_{1,e,h,\ p.u.} & 0 \\ 0 & 0 & Z_{2,e,h,\ p.u.} \end{bmatrix} \tag{41}$$

$$[Z_{abc,r,h}] = [A]^{-1}[Z_{012,r,h}][A] \tag{42}$$

The harmonic current of the referent node is equal to the total current injected into the network, for each harmonic order h. The total injected current is calculated as the sum of currents that flow through elements that connect referent and other nodes of an observed network. When the network is balanced, the nodal harmonic current is calculated using (43), and when the network is unbalanced the nodal harmonic current is calculated with (44).

$$I_{r,h} = \sum_{r:r\to n} I_{r,n,h} \tag{43}$$

$$I_{p,r,h} = \sum_{p,r:r\to n} I_{p,r,n,h} \tag{44}$$

Even though calculating the harmonic current of the referent node can be simplified using (45) and (46) in cases when only a positive sequence system is observed, when there are no transformers in a network or their vector group is e.g., Yy0. However, this simplification fails when a vector group of a transformer blocks zero sequence current, e.g., a vector group is Dyn. Therefore it can be used in a limited number of analyses, and it is not used in the implementation of the described mathematical model. The calculation of harmonic current is necessary for each element so that the current of the referent node can be determined.

$$I_{r,h} = \sum_{n=1}^{N} I_{n,h} \tag{45}$$

$$I_{p,r,h} = \sum_{n=1}^{N} I_{p,n,h} \tag{46}$$

When the harmonic impedance and the nodal current of the referent node are calculated, the referent node harmonic voltage for every harmonic order h is calculated with (47) for balanced power systems and (48) for unbalanced power systems.

$$U_{r,h} = Z_{r,h} \cdot I_{r,h} \tag{47}$$

$$[U_{abc,r,h}] = [Z_{abc,r,h}] \cdot [I_{r,p,h}] \tag{48}$$

After the voltage of the referent node and voltage drops for every other node are calculated, the nodal voltage for every harmonic order is created using (49) and (50).

$$U_{n,h} = U_{r,h} - \Delta U_{n,h} \tag{49}$$

$$[U_{abc,n,h}] = [U_{abc,r,h}] - [\Delta U_{abc,n,h}] \tag{50}$$

From nodal harmonic voltages, the system harmonic nodal voltage vector is created for balanced (51) and unbalanced power systems (52) and (53).

$$[U_h] = \begin{bmatrix} U_{1,h} \\ \vdots \\ U_{n,h} \end{bmatrix} \tag{51}$$

$$[U_{abc,h}] = \begin{bmatrix} [U_{abc,1,h}] \\ \vdots \\ [U_{abc,n,h}] \end{bmatrix} \tag{52}$$

$$[U_{abc,n,h}] = \begin{bmatrix} U_{a,n,h} \\ U_{b,n,h} \\ U_{c,n,h} \end{bmatrix} \tag{53}$$

It is important to mention that the calculation of harmonic voltage drop described by the above equations is not the only possible approach in harmonic analyses. Similar to power flow calculations, there are other methods, e.g., backward-forward-based methods, that can be used in the harmonic pollution assessment. The implementation of such methods is planned for the future upgrades of the tool presented in this paper.

When the values of the harmonic voltages are determined, it is possible to determine $THD_{n,u}$ for every node of the observed network (54), defined in the standards [47], 48]. This approach can be extended to the calculation of THD_u of each phase in unbalanced distribution networks.

$$THD_{u,n} = \sqrt{\sum_{h=2}^{H} \left(\frac{U_{n,h}}{U_1}\right)^2} \tag{54}$$

The majority of the description of the mathematical model is related to the calculation of node harmonic voltages. However, harmonic currents can potentially cause problems in distribution networks. Therefore, some of the European standards [47,48] also focus on current total harmonic distortion (THD_i). Calculation of harmonic current at each node is already described with Eqs. (16)–(26). From the calculated node currents, it is possible to calculate $THD_{i,n}$ for each node of a network (55). Similar to the voltage-related calculation of THD, after a small modification, Eq. (55) can be used in analyses of unbalanced distribution networks.

$$THD_{i,n} = \sqrt{\sum_{h=2}^{H} \left(\frac{I_{n,h}}{I_1}\right)^2} \tag{55}$$

3. Verification and test cases

As an update to pandapower, the developed harmonic analysis tool is verified against commercial tools NEPLAN and DigSILENT Power Factory. To compare the results, four test cases were created. To verify all three developed versions of the tool, a case of the balanced harmonic analysis considering only positive sequence (Type I), considering all sequence systems (Type II), and the unbalanced harmonic analysis (Type III) are developed. The balanced harmonic analysis functionality is defined differently in Power Factory compared to NEPLAN and the tool presented in this paper. It is not possible to observe all three sequence systems under the balanced condition, and therefore the developed tool could be verified against Power Factory only for Type I analysis.

The verification of the tool is made by determining the deviation between the results calculated by the tool presented in this paper and commercial tools NEPLAN and Power Factory. The deviation is defined as an absolute value of the difference of the results calculated by both tools. The deviations between the results of each phase, each node, and each harmonic order are compared, but only the maximum, minimum, and median deviations are presented in this paper. Generally, the deviation is calculated as an absolute value between the results obtained by the developed and a commercial tool,r according to equation (56):

$$\Delta_{tools} = \left| v_{n,p,h\ referent} - v_{n,p,h\ pandapower} \right| \tag{56}$$

where Δ_{tools} is the deviation between two tools, $v_{n,p,h\ referent}$ is the referent value determined with NEPLAN or Power Factory, and $v_{n,p,h\ pandapower}$ is the value calculated with the tool developed as the pandapower extension and presented in this paper.

The maximum deviation is calculated as the maximum value between all calculated deviations, both for THD values and harmonic voltages. Similarly, the minimum deviation is taken as the lowest

difference between values calculated by the tools. The third observed deviation is calculated as the median value of all determined deviations.

To validate the developed tool, four different test cases were created. Each of the test cases represents a radial balanced or unbalanced distribution network.

3.1. Test Case I

A simple three-bus MV network was created where the external grid is connected to the first node of the network, and the loads are three-phase connected to the two remaining nodes. The topology of the network is presented in Fig. 1. Both loads are defined as the harmonic source, i.e., they are injecting harmonic current in the network.

Table 1 shows the deviation between THD_u, U_h THD_i, and I_h calculated with the developed tool and commercial tools.

The results of the verification show no deviation larger than 0.01% when two tools are compared. The harmonic voltages are the same for every node and frequency, only when calculating THD a small difference occurs in some nodes. In the case of currents, both higher order harmonic currents and THD are the same for every node. Despite the small and insignificant deviation, the tested network is simple and before using the developed tool for analyses of larger, more complex networks it should be further validated.

3.2. Test Case II

A synthetic network defined by Kerber [49] is used for the verification of the developed tool. The topology of the network is presented in Fig. 2. The network consists of the external grid connected to the 10 kV node, transformer, 17 0.4 kV node, and lines that connect nodes. The loads are connected to eight nodes, and each load is defined as the harmonic source.

As mentioned before, a transformer's vector group plays a significant role in harmonic calculations. Therefore, to verify the precision of the developed tool, the comparison is made for two different vector groups, YNyn0 and Dyn5.

As it can be seen from the comparison shown in Table 2, values of deviation between developed and commercial tools are negligible, no matter the type or a transformer vector group. Both maximum and median differences between the results are not higher than 0.01%. Since the deviation is insignificant and it could be numeric, the results of the analysis and verification can lead to a conclusion that the developed tool can be used in harmonic analyses with different models of a transformer.

3.3. Test Case III

The networks presented in Test Case I and Test Case II are networks with only one or two voltage levels. As today distribution networks are moving towards smart, active distribution networks there is a possibility of reverse power flows and the propagation of PQ related problems from a lower voltage part to a higher voltage part of the network, i.e., the problems that occur in the distribution network can reflect in the transmission network. Therefore, the developed tool must be capable to work with more voltage levels. The network presented in Fig. 3 consists of 110, 10, and 0.4 kV nodes, two transformers, and lines connecting nodes. The loads are connected to both MV and LV nodes and are assumed to be harmonic sources.

As in the previous test case, both Type I and Type II analyses were made. For Type II, the results were compared for two different vector groups, YNyn0 and Dyn5. The comparison presented in Table 3 shows no significant differences in results of calculated harmonic voltages and THD_u that would make the developed tool unfit for planning and operation of power systems with multiple voltage levels. Even though the maximum deviation in some cases is slightly larger compared to the other cases and analyses, it can be determined as an outlier value, since the median deviation is not larger than 0.03% in the worst-case scenario. Current-related values do not present the problem since there is no difference in values calculated by the developed and commercial tools.

Fig. 1. Simple three-bus network.

3.4. Test Case IV

Networks presented in Test Case I, Test Case II, and Test Case III are defined as balanced distribution networks. LV networks are usually three-phase unbalanced networks and even though end-users can be single-phase or three-phase connected to the network, most of the end-users equipment is single-phase connected to the network. The benchmark CIGRE LV network defined by Strunz et al. [50] was modified and used for simulations and the verification of the developed tool. The network used for the verification in Test Case IV is presented in Fig. 4. Similar to previous cases, two vector groups were chosen, YNyn0 and Dyn5. Since the unbalanced harmonic calculation with the YNyn0 vector group is straightforward, the Dyn5 vector group is chosen since its model blocks the zero sequence current. Therefore, an implementation for that and similar vector groups is more challenging and additional functionalities must be implemented in order to keep the precision of the tool.

Table 4 shows the deviation between values calculated with the commercial tool and with the developed open source approach. The deviation between tools for the unbalanced analysis is higher compared to previous cases, especially when the vector group of a transformer is Dyn5 due to simplification in a transformer group modeling. However, even in the case of Dyn5, the value of median deviation is insignificant and does not impact the usability of the newly developed tool. When the tool is compared to Power Factory, the maximum deviation is significantly higher. However, this deviation is only an outlier value calculated for only one node, phase, and frequency. Additionally, the median deviation is lower and is only slightly higher than the deviation between the developed tool and NEPLAN. It is important to mention that every tool has its own characteristics, the precise definition of input data, and the mathematical model of the network. Due to the differences, it is possible that at some nodes or frequencies the deviations are larger. In spite of deviations, the results show no deviations in further use of the developed tool in harmonic analysis.

In all previous cases, only one harmonic source was connected to each phase or each node. Since the number of end-users with installed LC technologies is increasing and there are multiple harmonic sources connected to different phases and nodes there is a need for verification of the calculation in cases when there are multiple harmonic sources in the phase or node. A modified CIGRE LV network was used to verify the developed tool in the case when end-users have installed PVs, i.e., more than one harmonic source is connected to a certain node.

The results of the comparison presented in Table 5 are similar to the results of the analysis in which end-users did not have installed PVs. Even though the deviation occurs, the values are within acceptable boundaries and the difference in the results calculated with two tools does not significantly deteriorate the precision of the tool. When observing the values of comparison with the Power Factory commercial tool, the values are significantly higher than the values of comparison with NEPLAN. However, it is important to mention that such differences occur even when two commercial tools are compared. Each tool has its characteristics and to further decrease the deviation, a detailed mathematical model and the way of defining input data needed for the harmonic analysis should be investigated. Even though the maximum deviation is high, values of minimum and median deviation show that the developed tool is accurate and could be used in future analyses. This is important from the aspect of LV network operation, which is becoming more demanding since the number of end-users with installed

Table 1
Deviation between tools (absolute values) - Test Case I.

Harmonics-related quantity	Minimum deviation (%) - NEPLAN	Minimum deviation (%) - Power factory	Maximum deviation (%) - NEPLAN	Maximum deviation (%) - Power factory	Median deviation (%) - NEPLAN	Median deviation (%) - Power factory
U_h - Type I	0.00	0.00	0.00	0.00	0.00	0.00
THD_u - Type I	0.00	0.00	0.01	0.01	0.00	0.01
U_h - Type II	0.00	–	0.00	–	0.00	–
THD_u - Type II	0.00	–	0.01	–	0.01	–
I_h - Type I	0.00	0.00	0.00	0.00	0.00	0.00
THD_i - Type I	0.00	0.00	0.00	0.00	0.00	0.00
I_h - Type II	0.00	–	0.00	–	0.00	–
THD_i - Type II	0.00	–	0.00	–	0.00	–

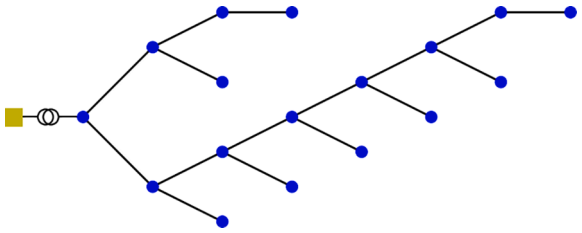

Fig. 2. Kerber synthetic network.

PVs or EV charging stations is increasing. The verification of cases in which more than one harmonic source is connected to a node is an important step in using the tool for further analyses of the power systems, especially LV networks with the increasing share of PVs, EVs, battery storage, and other LC units.

4. Application of the tool - Integration of DERs

The main motivation behind the development of the tool was enabling an easy and quick assessment of harmonic pollution in smart, active distribution networks. Since the share of EVs is constantly increasing and an installment of PVs is becoming more profitable, the number of end-users that decide to invest in LC units is growing. Both PVs and home EV charging stations are connected via power electronic devices to a network, and power electronic devices are one of the largest harmonic polluters in distribution networks. Besides LC units, already existing non-linear loads installed at the places of final consumption cause problems related to harmonic distortion. To additionally show the possibilities of the tool but also to show the importance of the development of such tools, a real-world case study is created in Section 4.

A network that represents Croatian urban LV feeder is defined and shown in Fig. 5. A case study is defined so that the impact of users with installed DERs on harmonic distortion can be realistically determined. Devices of every end-user connected to the network are considered as a harmonic source. Additionally, depending on the defined scenario, the different share of end-users have installed PVs and EV charging stations. Three different scenarios are created, mimicking the targets set by the EU for 2030 and 2050. In Scenario 1, none of the end-users have installed LC units. In 2030, 40% of energy should be produced from renewable energy sources [51]. Therefore, in Scenario 2 40% of end-users have installed PVs and EV charging stations at their households. A long-term plan defined in ACl [52] sets the target of energy production from RESs to more than 80%. Following the logic, Scenario 3 is defined as one in which 80% of end-users have installed PVs and EV charging stations.

Since every end-user is considered as a harmonic polluter, the residential harmonic spectra are created according to Niitsoo et al. [53], Mazin et al. [54]. The harmonic curves related to a PV production are made based on those defined in paper [55], while the harmonic spectra of an EV charging are based on the data collected from metering infrastructure installed in charging stations in Croatia. The power curve of an EV charging is created with the goal of minimizing the cost of participating in the day-ahead electricity market, while end-users consumption and PV production curves are created based on the data collected from smart meters. PVs and EV charging stations are single-phase connected to the network, and their connection phase is randomly selected since it

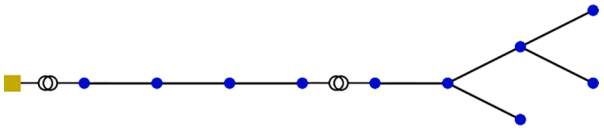

Fig. 3. HV-MV-LV test network.

Table 2
Deviation between tools (absolute values) - Test Case II.

Harmonics-related quantity	Minimum deviation (%) - NEPLAN	Minimum deviation (%) - Power factory	Maximum deviation (%) - NEPLAN	Maximum deviation (%) - Power factory	Median deviation (%) - NEPLAN	Median deviation (%) - Power factory
U_h - Type I	0.00	0.00	0.01	0.00	0.00	0.00
THD_u - Type I	0.00	0.00	0.01	0.00	0.01	0.00
U_h -Type II - YNyn0	0.00	–	0.01	–	0.00	–
THD_u - Type II - YNyn0	0.00	–	0.01	–	0.00	–
U_h - Type II - Dyn5	0.00	–	0.01	–	0.01	–
THD_u - Type II - Dyn5	0.00	–	0.01	–	0.00	–
I_h - Type I	0.00	0.00	0.00	0.00	0.00	0.00
THD_i - Type I	0.00	0.00	0.00	0.00	0.00	0.00
I_h - Type II - YNyn0	0.00	–	0.00	–	0.00	–
THD_i - Type II - YNyn0	0.00	–	0.00	–	0.00	–
I_h - Type II - Dyn5	0.00	–	0.00	–	0.00	–
THD_i - Type II - Dyn5	0.00	–	0.00	–	0.00	–

Table 3
Deviation between tools (absolute values) - Test Case III.

Harmonics-related quantity	Minimum deviation (%) - NEPLAN	Minimum deviation (%) - Power factory	Maximum deviation (%) - NEPLAN	Maximum deviation (%) - Power factory	Median deviation (%) - NEPLAN	Median deviation (%) - Power factory
U_h - Type I	0.00	0.00	0.00	0.00	0.00	0.00
THD_u - Type I	0.00	0.00	0.00	0.00	0.00	0.00
U_h - Type II - YNyn0	0.00	–	0.03	–	0.00	–
THD_u - Type II - YNyn0	0.00	–	0.03	–	0.03	–
U_h - Type II - Dyn5	0.00	–	0.10	–	0.01	–
THD_u - Type II - Dyn5	0.00	–	0.03	–	0.00	–
I_h - Type I	0.00	0.00	0.00	0.00	0.00	0.00
THD_i - Type I	0.00	0.00	0.00	0.00	0.00	0.00
I_h - Type II - YNyn0	0.00	–	0.00	–	0.00	–
THD_i - Type II - YNyn0	0.00	–	0.00	–	0.00	–
I_h - Type II - Dyn5	0.00	–	0.00	–	0.00	–
THD_i - Type II - Dyn5	0.00	–	0.00	–	0.00	–

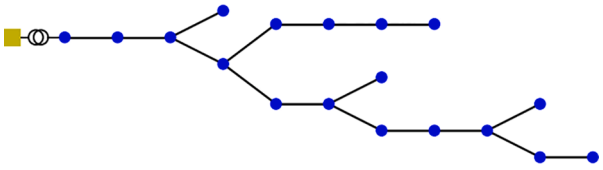

Fig. 4. Modified benchmark CIGRE LV network.

presents the realistic case in which end-users do not know the phase to which their devices are connected.

Harmonic analysis is made for one week period and the results of the analysis are shown in Fig. 6.

The analysis of the results shows a trend of increase of THD value with the integration of LC units. Even though the value of THD in phase A in Scenario 1 violates the limitation of 8%, a violation does not happen in more than 5% intervals, which is in accordance with different European standards and national grid codes [47,48]. Since it is expected that the share and installed power of LC units continues to grow, the

Table 4
Deviation between tools (absolute values) - Test Case IV.

Harmonics-related quantity	Minimum deviation (%) - NEPLAN	Minimum deviation (%) - Power factory	Maximum deviation (%) - NEPLAN	Maximum deviation (%) - Power factory	Median deviation (%) - NEPLAN	Median deviation (%) - Power factory
U_h - Type III - YNyn0	0.00	0.00	0.01	1.19	0.00	0.19
THD_u - Type III - YNyn0	0.00	0.12	0.00	0.29	0.00	0.21
U_h - Type III - Dyn5	0.00	0.00	0.27	0.85	0.13	0.09
THD_u - Type III - Dyn5	0.00	0.00	0.22	1.34	0.06	0.25
I_h - Type III - YNyn0	0.00	0.00	0.00	0.00	0.00	0.00
THD_i - Type III - YNyn0	0.00	0.00	0.00	0.00	0.00	0.00
I_h - Type III - Dyn5	0.00	0.00	0.00	0.00	0.00	0.00
THD_i - Type III - Dyn5	0.00	0.00	0.00	0.00	0.00	0.00

Table 5
Deviation between tools (absolute values) - Test Case IV - with connected PVs.

Harmonics-related quantity	Minimum deviation (%) - NEPLAN	Minimum deviation (%) - Power factory	Maximum deviation (%) - NEPLAN	Maximum deviation (%) - Power factory	Median deviation (%) - NEPLAN	Median deviation (%) - Power factory
U_h - Type III - YNyn0	0.00	0.00	0.02	1.12	0.02	0.22
THD_u - Type III - YNyn0	0.00	0.12	0.03	0.29	0.01	0.23
U_h - Type III - Dyn5	0.00	0.00	0.27	0.83	0.13	0.10
THD_u - Type III - Dyn5	0.00	0.00	0.20	1.46	0.06	0.17
I_h - Type III - YNyn0	0.00	0.00	0.00	0.00	0.00	0.00
THD_i - Type III - YNyn0	0.00	0.00	0.00	0.00	0.00	0.00
I_h - Type III - Dyn5	0.00	0.00	0.00	0.00	0.00	0.00
THD_i - Type III - Dyn5	0.00	0.00	0.00	0.00	0.00	0.00

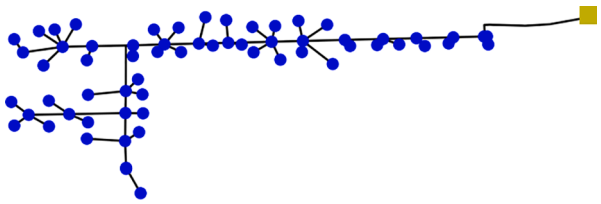

Fig. 5. Real-world LV circuit.

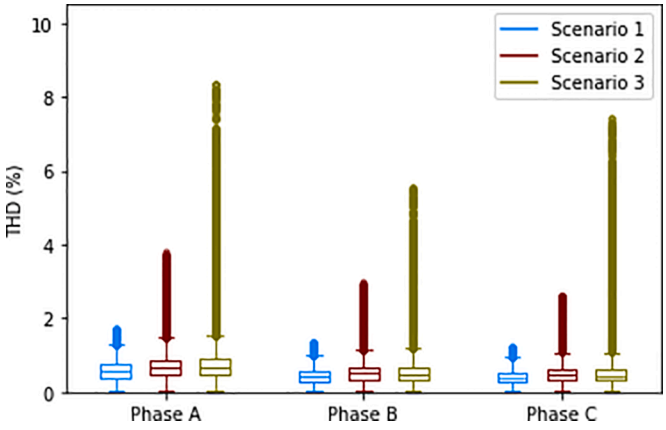

Fig. 6. Results of a real-world LV network harmonic analysis.

harmonics-related problems will only increase. This additionally emphasizes the importance of tools like the one presented in this paper, since it enables simple and quick calculations of complex power systems. The contribution of the paper is an implementation of the mathematical model and verification of the developed tool, and not finding a method that will help DSOs ins preventing and mitigating the problems related to harmonic distortion. However the open-source formulation, available at [39], simplifies further upgrades of the tool and potentially enables the integration of algorithms that will be used in the decrease or even mitigation of harmonic pollution.

5. Conclusions and future work

In order to overcome the intensive changes occurring due to power system decarbonization, the tools for the power system analyses need to be adaptable, expandable, and flexible. Having them openly available to a broader community creates opportunities for the development of new features and ideas and thus speeds up the transition toward a zero-emission society.

A detailed literature review identified that the existing open source tools often lack important technical analysis capabilities and mathematical explanations of how they are modeled and integrated. This hinders further development and analyses. To bridge this gap we develop an upgrade to an open source tool pandapower, an existing Python-based tool for analyses of steady-state power systems. The balanced and unbalanced harmonic analyses tool, soon to be implemented as a part of pandapower, is made freely available at [39], while technical and mathematical aspects of developing the tool are explained in the paper for the first time.

Three types of harmonic analysis were developed, two for balanced radial distribution systems, and one for three-phase unbalanced systems. The validation against commercial software shows negligible differences for the same defined test cases. After the verification, all benefits of the tool are shown on the additional test case that represents a real-world LV network.

Further upgrade of the tool includes full implementation in the pandapower library and the improvement of the accuracy, using more precise models of some elements, expansion with additional analyses, and verification of other, more complex test cases. Since the focus of the current version of the developed tool was put on distribution networks, which are in most cases operated radially, the mathematical model is not valid for the calculations of meshed networks. Further upgrades of the tool include an implementation of a method that is valid also for meshed grids. Backward-forward-based methods, which are planned to be implemented in future versions of the tool, are able to work both with radial and meshed grids but could also potentially contribute to increasing the tool's accuracy and speed, which is especially important for time-series analyses. Also, the developed tool can be used in numerous analyses, e.g., in determining the impact of a transformer vector group on PQ parameters, and in the planning and operation of smart distribution networks. An open source approach even enables the implementation of optimization or similar algorithms that will help DSOs in mitigating harmonics-related problems in distribution networks and guarantee success with further integration of LC technologies.

Funding

The work is supported in part by Croatian Science Foundation (HRZZ) and Croatian Distribution System Operator (HEP ODS) under the project IMAGINE - Innovative Modelling and Laboratory Tested Solutions for Next Generation of Distribution Networks (PAR-2018-12) and in part by the European Structural and Investment Funds under project KK.01.2.1.02.0042 DINGO (Distribution Grid Optimization).

CRediT authorship contribution statement

Tomislav Antić: Conceptualization, Methodology, Software, Validation, Formal analysis, Investigation, Writing – original draft, Writing – review & editing, Visualization. **Leon Thurner:** Software, Validation, Data curation, Writing – review & editing. **Tomislav Capuder:** Conceptualization, Methodology, Writing – original draft, Writing – review & editing, Visualization, Supervision, Funding acquisition. **Ivica Pavić:** Conceptualization, Methodology, Resources, Supervision.

Declaration of Competing Interest

The authors declare that they have no known competing financial interests or personal relationships that could have appeared to influence the work reported in this paper.

References

[1] International Renewable Energy Agency, Renewable Energy Capacity Statistics 2021. Technical Report, International Renewable Energy Agency, Abu Dhabi, 2021.https://www.irena.org/publications/2021/March/Renewable-Capacity-Statistics-2021

[2] A. Jäger-Waldau, PV Status Report 2019. Technical Report, Publications Office of the European Union: Luxembourg, 2019.https://ec.europa.eu/jrc/sites/jrcsh/files/kjna29938enn_1.pdf

[3] J. von Appen, M. Braun, T. Stetz, K. Diwold, D. Geibel, Time in the sun: the challenge of high PV penetration in the German electric grid, IEEE Power Energy Mag. 11 (2) (2013) 55–64, https://doi.org/10.1109/MPE.2012.2234407.

[4] I.R.E. Agency, Electricity Storage and Renewables: Costs and Markets to 2030. Technical Report, International Renewable Energy Agency, Abu Dhabi, 2017.https://www.irena.org/publications/2017/Oct/Electricity-storage-and-renewables-costs-and-markets

[5] L. Maeyaert, L. Vandevelde, T. Döring, Battery storage for ancillary services in smart distribution grids, J. Energy Storage 30 (2020) 101524, https://doi.org/10.1016/j.est.2020.101524.

[6] R. Tonkoski, L.A.C. Lopes, T.H.M. El-Fouly, Coordinated active power curtailment of grid connected PV inverters for overvoltage prevention, IEEE Trans. Sustain. Energy 2 (2) (2011) 139–147, https://doi.org/10.1109/TSTE.2010.2098483.

[7] A. Asrari, M. Ansari, J. Khazaei, P. Fajri, A market framework for decentralized congestion management in smart distribution grids considering collaboration among electric vehicle aggregators, IEEE Trans. Smart Grid 11 (2) (2020) 1147–1158, https://doi.org/10.1109/TSG.2019.2932695.

[8] X. Liang, C. Andalib Bin-Karim, Harmonics and mitigation techniques through advanced control in grid-connected renewable energy sources: a review, IEEE

Trans. Ind. Appl. 54 (4) (2018) 3100–3111, https://doi.org/10.1109/TIA.2018.2823680.
[9] T. Antić, T. Capuder, M. Bolfek, A comprehensive analysis of the voltage unbalance factor in PV and EV rich non-synthetic low voltage distribution networks, Energies 14 (1) (2021), https://doi.org/10.3390/en14010117.
[10] K. Mahmud, A.K. Sahoo, E. Fernandez, P. Sanjeevikumar, J.B. Holm-Nielsen, Computational tools for modeling and analysis of power generation and transmission systems of the smart grid, IEEE Syst. J. 14 (3) (2020) 3641–3652, https://doi.org/10.1109/JSYST.2020.2964436.
[11] K. Mahmud, G.E. Town, A review of computer tools for modeling electric vehicle energy requirements and their impact on power distribution networks, Appl. Energy 172 (2016) 337–359, https://doi.org/10.1016/j.apenergy.2016.03.100.
[12] M. Zain ul Abideen, O. Ellabban, L. Al-Fagih, A review of the tools and methods for distribution networks' hosting capacity calculation, Energies 13 (11) (2020), https://doi.org/10.3390/en13112758.
[13] L.I. Dulău, D. Bică, Power flow analysis with loads profiles, Procedia Eng. 181 (2017) 785–790, https://doi.org/10.1016/j.proeng.2017.02.466.10th International Conference Interdisciplinarity in Engineering, INTER-ENG 2016, 6-7 October 2016, Tirgu Mures, Romania
[14] A. Sani Hassan, L. Cipcigan, N. Jenkins, Impact of optimised distributed energy resources on local grid constraints, Energy 142 (2018) 878–895, https://doi.org/10.1016/j.energy.2017.10.074.
[15] J.P. Holguin, D.C. Rodriguez, G. Ramos, Reverse power flow (RPF) detection and impact on protection coordination of distribution systems, IEEE Trans. Ind. Appl. 56 (3) (2020) 2393–2401, https://doi.org/10.1109/TIA.2020.2969640.
[16] S.R.K. Najafabadi, B. Fani, I. Sadeghkhani, Optimal determination of photovoltaic penetration level considering protection coordination, IEEE Syst. J. (2021) 1–4, https://doi.org/10.1109/JSYST.2021.3052527.
[17] M.T. Turan, Y. Ates, O. Erdinc, E. Gokalp, J.P.S. Catalão, Effect of electric vehicle parking lots equipped with roof mounted photovoltaic panels on the distribution network, Int. J. Electr. Power Energy Syst. 109 (2019) 283–289, https://doi.org/10.1016/j.ijepes.2019.02.014.
[18] S. Khatua, V. Mukherjee, Adaptive overcurrent protection scheme suitable for station blackout power supply of nuclear power plant operated through an integrated microgrid, Electr. Power Syst. Res. 192 (2021) 106934, https://doi.org/10.1016/j.epsr.2020.106934.
[19] S. Maharjan, D. Sampath Kumar, A.M. Khambadkone, Enhancing the voltage stability of distribution network during PV ramping conditions with variable speed drive loads, Appl. Energy 264 (2020) 114733, https://doi.org/10.1016/j.apenergy.2020.114733.
[20] B.B. Adetokun, J.O. Ojo, C.M. Muriithi, Reactive power-voltage-based voltage instability sensitivity indices for power grid with increasing renewable energy penetration, IEEE Access 8 (2020) 85401–85410, https://doi.org/10.1109/ACCESS.2020.2992194.
[21] D. Chathurangi, U. Jayatunga, M. Rathnayake, A. Wickramasinghe, A. Agalgaonkar, S. Perera, Potential power quality impacts on LV distribution networks with high penetration levels of solar PV. 2018 18th International Conference on Harmonics and Quality of Power (ICHQP), 2018, pp. 1–6, https://doi.org/10.1109/ICHQP.2018.8378890.
[22] L. Thurner, A. Scheidler, F. Schäfer, J.-H. Menke, J. Dollichon, F. Meier, S. Meinecke, M. Braun, Pandapower-an open-source python tool for convenient modeling, analysis, and optimization of electric power systems, IEEE Trans. Power Syst. 33 (6) (2018) 6510–6521, https://doi.org/10.1109/TPWRS.2018.2829021.
[23] L. Thurner, M. Braun, Vectorized calculation of short circuit currents considering distributed generation—An open source implementation of IEC 60909. 2018 IEEE PES Innovative Smart Grid Technologies Conference Europe (ISGT-Europe), 2018, pp. 1–6, https://doi.org/10.1109/ISGTEurope.2018.8571529.
[24] S.H. Oh, Y.T. Yoon, S.W. Kim, Online reconfiguration scheme of self-sufficient distribution network based on a reinforcement learning approach, Appl. Energy 280 (2020) 115900, https://doi.org/10.1016/j.apenergy.2020.115900.
[25] R.D. Zimmerman, C.E. Murillo-Sánchez, R.J. Thomas, MATPOWER: steady-state operations, planning, and analysis tools for power systems research and education, IEEE Trans. Power Syst. 26 (1) (2011) 12–19, https://doi.org/10.1109/TPWRS.2010.2051168.
[26] M. Nemati, M. Braun, S. Tenbohlen, Optimization of unit commitment and economic dispatch in microgrids based on genetic algorithm and mixed integer linear programming, Appl. Energy 210 (2018) 944–963, https://doi.org/10.1016/j.apenergy.2017.07.007.
[27] V. Suresh, N. Bazmohammadi, P. Janik, J.M. Guerrero, D. Kaczorowska, J. Rezmer, M. Jasinski, Z. Leonowicz, Optimal location of an electrical vehicle charging station in a local microgrid using an embedded hybrid optimizer, Int. J. Electr. Power Energy Syst. 131 (2021) 106979, https://doi.org/10.1016/j.ijepes.2021.106979.
[28] D. Thomas, G. D'Hoop, O. Deblecker, K.N. Genikomsakis, C.S. Ioakimidis, An integrated tool for optimal energy scheduling and power quality improvement of a microgrid under multiple demand response schemes, Appl. Energy 260 (2020) 114314, https://doi.org/10.1016/j.apenergy.2019.114314.
[29] S.F. Abdelsamad, W.G. Morsi, T.S. Sidhu, Impact of wind-based distributed generation on electric energy in distribution systems embedded with electric vehicles, IEEE Trans. Sustain. Energy 6 (1) (2015) 79–87, https://doi.org/10.1109/TSTE.2014.2356551.
[30] J.H. Angelim, C. de Mattos Affonso, Probabilistic assessment of voltage quality on solar-powered electric vehicle charging station, Electr. Power Syst. Res. 189 (2020) 106655, https://doi.org/10.1016/j.epsr.2020.106655.
[31] T. Morstyn, K.A. Collett, A. Vijay, M. Deakin, S. Wheeler, S.M. Bhagavathy, F. Fele, M.D. McCulloch, OPEN: an open-source platform for developing smart local energy system applications, Appl. Energy 275 (2020) 115397, https://doi.org/10.1016/j.apenergy.2020.115397.
[32] M. Chamana, K. Prabakar, B. Palmintier, M.M. Baggu, Conversion and validation of distribution system model from a QSTS-based tool to a real-time dynamic phasor simulator. 2017 Ninth Annual IEEE Green Technologies Conference (GreenTech), 2017, pp. 219–225, https://doi.org/10.1109/GreenTech.2017.38.
[33] W. Xu, Component modeling issues for power quality assessment, IEEE Power Eng. Rev. 21 (11) (2001) 12–17, https://doi.org/10.1109/MPER.2001.961998.
[34] T. Modeling, Modeling and simulation of the propagation of harmonics in electric power networks. I. Concepts, models, and simulation techniques, IEEE Trans. Power Deliv. 11 (1) (1996) 452–465, https://doi.org/10.1109/61.484130.
[35] T. Modeling, Modeling and simulation of the propagation of harmonics in electric power networks. II. Sample systems and examples, IEEE Trans. Power Deliv. 11 (1) (1996) 466–474, https://doi.org/10.1109/61.484131.
[36] A. Medina, J. Segundo-Ramirez, P. Ribeiro, W. Xu, K.L. Lian, G.W. Chang, V. Dinavahi, N.R. Watson, Harmonic analysis in frequency and time domain, IEEE Trans. Power Deliv. 28 (3) (2013) 1813–1821, https://doi.org/10.1109/TPWRD.2013.2258688.
[37] F.L. Vieira, P.F. Ribeiro, B.D. Bonatto, T.E.C. Oliveira, Harmonic studies in openDSS considering renewable DG and aggregate linear load models. 2018 13th IEEE International Conference on Industry Applications (INDUSCON), 2018, pp. 202–207, https://doi.org/10.1109/INDUSCON.2018.8627343.
[38] H. Sharma, M. Rylander, D. Dorr, Grid impacts due to increased penetration of newer harmonic sources, IEEE Trans. Ind. Appl. 52 (1) (2016) 99–104, https://doi.org/10.1109/TIA.2015.2464175.
[39] pandapower GitHub repository - harmonic analysis, https://github.com/e2nIEE/pandapower/tree/harmonics.
[40] A. Koirala, R. D'Hulst, D. Van Hertem, Impedance modelling for European style Distribution Feeder. 2019 International Conference on Smart Energy Systems and Technologies (SEST) Porto, Portugal, 2019, https://doi.org/10.1109/SEST.2019.8849015.
[41] V. Ćuk, J.F.G. Cobben, W.L. Kling, P.F. Ribeiro, Considerations on harmonic impedance estimation in low voltage networks. 2012 IEEE 15th International Conference on Harmonics and Quality of Power, 2012, pp. 358–363, https://doi.org/10.1109/ICHQP.2012.6381250.
[42] J.R. Marti, Accurate modelling of frequency-dependent transmission lines in electromagnetic transient simulations, IEEE Trans. Power Appar. Syst. PAS-101 (1) (1982) 147–157, https://doi.org/10.1109/TPAS.1982.317332.
[43] B. Gustavsen, A. Semlyen, Rational approximation of frequency domain responses by vector fitting, IEEE Trans. Power Deliv. 14 (3) (1999) 1052–1061, https://doi.org/10.1109/61.772353.
[44] T. Zheng, E.B. Makram, A.A. Girgis, Evaluating power system unbalance in the presence of harmonic distortion, IEEE Trans. Power Deliv. 18 (2) (2003) 393–397, https://doi.org/10.1109/TPWRD.2002.807460.
[45] D.P. Manjure, E.B. Makram, Impact of unbalance on power system harmonics. 10th International Conference on Harmonics and Quality of Power (ICHQP) volume 1, 2002, pp. 328–333vol.1, https://doi.org/10.1109/ICHQP.2002.1221454.
[46] J. Arrillaga, N.R. Watson, Power System Harmonics, John Wiley & Sons Ltd., Chichester, West Sussex, England, 2003.
[47] IEC 61000-2-2 Electromagnetic compatibility (EMC) Part 2-2: Environment - Compatibility levels for low-frequency conducted disturbances and signalling in public low-voltage power supply systems, 2008a,.
[48] IEC 61000-2-12 Electromagnetic compatibility (EMC) Part 2-12 : Environment - Compatibility levels for low-frequency conducted disturbances and signalling in public medium-voltage power supply systems, 2008b,.
[49] G. Kerber. Capacity of Low Voltage Distribution Networks with Increased Feed-in of Photovoltaic Power, Technische Universität München, Munich, 2010. Ph.D. thesis.
[50] K. Strunz, E. Abbasi, R. Fletcher, N. Hatziargyriou, R. Iravani, G. Joos, TF C6.04.02 : TB 575 – Benchmark Systems for Network Integration of Renewable and Distributed Energy Resources, CIGRE, 2014.
[51] Delivering the European Green Deal, 2021, https://ec.europa.eu/info/strategy/priorities-2019-2024/european-green-deal/delivering-european-green-deal_en.
[52] A Clean Planet for all A European strategic long-term vision for a prosperous, modern, competitive and climate neutral economy, Technical Report, European Commission, Brussels, Belgium, 2018.
[53] J. Niitsoo, J. Kilter, I. Palu, P. Taklaja, L. Kütt, Harmonic levels of domestic and electrical vehicle loads in residential distribution networks. 2013 Africon, 2013, pp. 1–5, https://doi.org/10.1109/AFRCON.2013.6757800.
[54] H.E. Mazin, E.E. Nino, W. Xu, J. Yong, A study on the harmonic contributions of residential loads, IEEE Trans. Power Deliv. 26 (3) (2011) 1592–1599, https://doi.org/10.1109/TPWRD.2010.2096236.
[55] J. Niitsoo, P. Taklaja, I. Palu, J. Klüss, Power quality issues concerning photovoltaic generation and electrical vehicle loads in distribution grids, Smart Grid Renew. Energy 6 (6) (2015) 164–177, https://doi.org/10.4236/sgre.2015.66015.